Journal of Marine Research, 42, 787–808, 1984

Tidal period upwelling within Raine Island Entrance Great Barrier Reef

by Richard E. Thomson[1,2] and Eric J. Wolanski[1]

ABSTRACT

Temperature and current measurements collected from November 1981 to May 1982 at the head of Raine Island Entrance reveal tidally-induced upwelling of cold continental slope water onto the continental shelf. Daily tidal motions account for approximately 80% of the total cross-shelf eddy heat flux of 0.79 ± 1.01 cal cm^{-2} s^{-1}. Although temperature and current fluctuations are principally of semidiurnal period, the heat flux is principally at diurnal period. Based on empirical nutrient-temperature relations we estimate the onshore inorganic nutrient fluxes to be 0.9 (±1.2) × 10^{-2} mmol m^{-2} s^{-1} for nitrate, 0.6 (±0.8) × 10^{-2} mmol m^{-2} s^{-1} for silicate and 0.7 (±0.9) × 10^{-3} mmol m^{-2} s^{-1} for phosphate.

The upwelling is explained in terms of fluid withdrawal-type mechanisms in which nutrient-rich thermocline water below 100 m depth is drawn onto the shallow (40 m) shelf during the flood. We suggest that this tidal period inundation of the outer reefs is an important mechanism for effectively upgrading nominally low nutrient levels. Reef growth is expected to be most prolific near the shelf break where the time-integrated contribution of the upwelling is greatest.

1. Introduction

Shallow reefs occupy roughly 90% of the distance between 16.5 to 9.5S latitude along the shelf edge of northeast Australia (Pickard *et al.*, 1977). These reefs, in effect, form a 'porous' boundary that must certainly inhibit the movement of water between the outer shelf and the Coral Sea, but which may permit sufficient exchange through the passages to enable oceanically-derived nutrients to reach the outer lagoon. However, the well-mixed upper 100 m of the Coral Sea is low in nutrients so that more than a simple horizontal exchange and mixing of surface waters is required. This leads to the notion that nutrient enrichment of the reef zone is affected by upwelling onto the shelf of continental slope water from the depths of the subsurface thermocline.

That coral reef distribution may be linked to upwelling at continental shelf regions is not new to the literature (e.g., Orr, 1933). Maxwell and Swinchatt (1970) further suggest a correlation between prolific reef growth and steepness of the slope. What has yet to be established are the kinds and relative importances of processes capable of 'lifting' the offshore thermocline a height of 50 m onto the shelf break. Thompson and

1. Australian Institute of Marine Science, P.M.B. No. 3, Townsville, MOS, Qld., 4810, Australia.
2. Present address: Institute of Ocean Sciences, 9860 West Saanich Road, Sidney, British Columbia, Canada V8L 4B2.

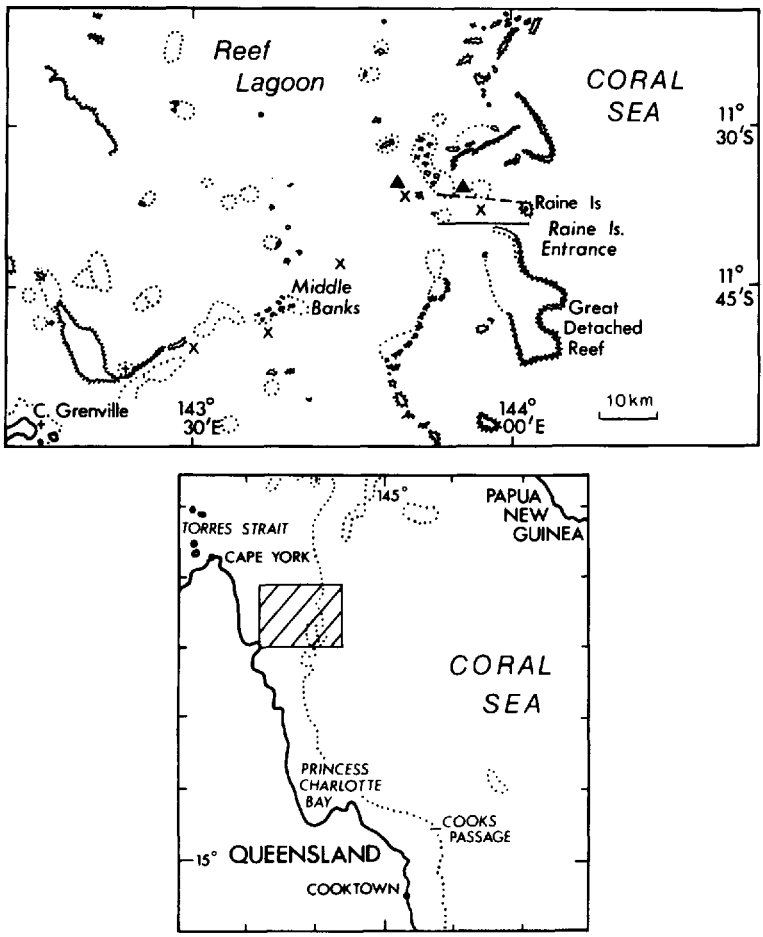

Figure 1. Region of Great Barrier Reef in the vicinity of Raine Island Entrance. Dotted line marks 10 fathom (18 m) contour. Triangles denote current meter moorings; x's are CTD stations. Insert shows study area in relation to the Queensland coast. Lines correspond to the sections in Figure 2. (Adapted from Australian Hydrographic Services, chart 1039).

Golding (1981) propose a mechanism based on modified potential flow in which flood currents accelerated through narrow reef passages draw nutrient-rich water onto the shelf from across the slope. More recently, Andrews and Gentien (1982) present observational results that indicate a correlation between intrusions onto the shelf of cold, nutrient-rich water and low frequency (order 90 day period) fluctuations in the East Australian Current. The latter are assumed to be associated with some large-scale oceanic phenomenon such as topographic Rossby waves (Garrett, 1979). Once on the shelf, nutrients are thought to be pumped into the lagoon via a bottom Ekman layer associated with wind-generated 30 day reversals in the alongshore component of the

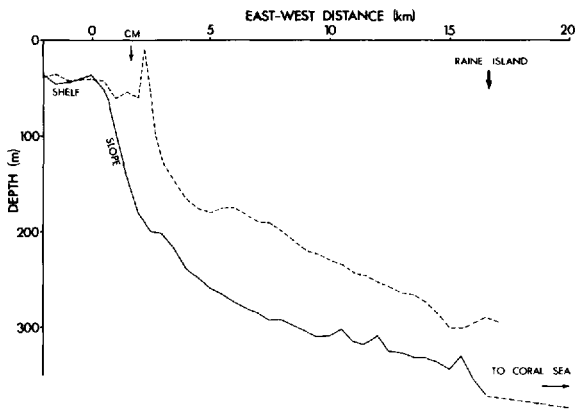

Figure 2. East-west bottom topography for two sections in Raine Island Entrance region (cf Fig. 1). CM marks the position of slope current meter mooring.

current. Finally, the results of Wolanski and Pickard (1983) suggest that semidiurnal baroclinic tides generated through the interaction of the alongshore component of the barotropic tidal current and the bottom topography near the shelf break off Myrmidon Reef may be important to the introduction of nutrients to the outer reef.

This paper deals with upwelling at the head of Raine Island Entrance, a basin-like incision normal to the shelf-edge at 11°38′ S latitude. Using more than five months of temperature and velocity records from instruments moored in the entrance and on the adjacent shelf (Section 2), we show that there are strong tidally-induced intrusions of cold, deeper water to the shelf and that the relationship between temperature and onshore flow can be explained by fluid withdrawal processes (Section 3). Section 3 also contains estimates of the eddy heat flux associated with the upwelling. Corresponding estimates of the nutrient fluxes are then based on empirical temperature-nutrient relations. Summary and conclusions are presented in Section 4.

2. Observations

Raine Island Entrance is part of a rectangular-shaped basin that cuts latitudinally about 20 km through the dense northern sector of the Great Barrier Reef (Fig. 1). The outer portion of the basin is some 20 km wide with depths of 300 to 400 m bordering a steep continental slope. The entrance shoals gradually along most of its axis and terminates at a comparatively reef-free shelf-edge. Immediately prior to the shelf there is a marked decrease in depth from 200 m to less than 50 m at typical mean slopes of about 0.1 (Fig. 2).

Single Aanderaa RCM 4 current meters were moored at two locations near the head of the entrance from 15 November 1981 to 1 May 1982. The seaward meter was at 105 m depth in 150 m of water on the slope approximately 13 km west of Raine Island; the other meter was on the shelf a further 10 km west at 35 m depth in 40 m of water.

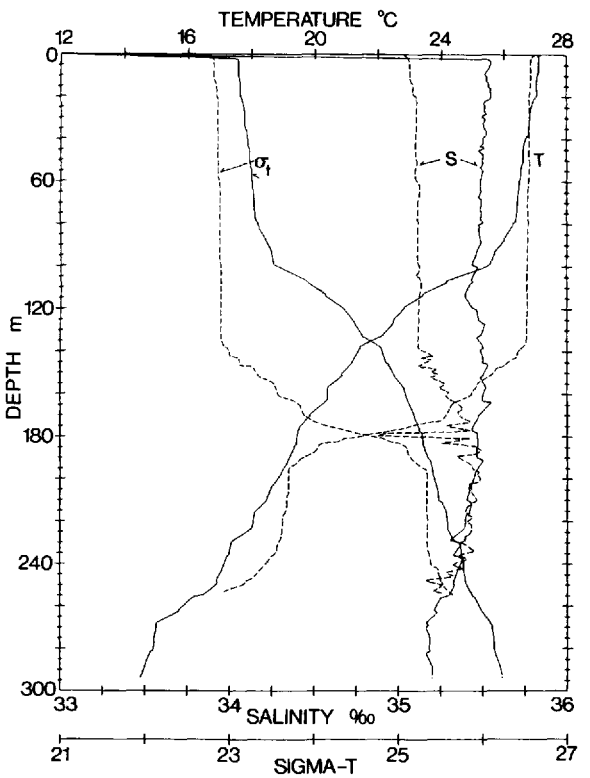

Figure 3. Profiles of temperature (T), salinity (S) and density (σ_t) near Raine Island. Solid lines, November 16, 1981. Dashed lines, May 1, 1982.

Records consisted of half-hourly values of averaged speed plus instantaneous values of current direction and *in situ* temperature. A gap in the speed record at the shelf mooring between 15–21 March 1982 (due to a "stuck" rotor) has been bridged using predicted tidal current constituents obtained from the entire length of record. Conductivity was also measured although growth on the induction cell lead to dubious long-term values. Hourly winds and air temperature were obtained from an Aanderaa 'weather' recorder on Raine Island and half-hourly sea levels from Aanderaa pressure recorders near the island and at Middle Banks 50 km to the west (Fig. 1). In addition, STD profiles were taken across the shelf and in the vicinity of the moorings at the times of deployment and recovery.

a. Water property distributions. Representative profiles of temperature, salinity and density (sigma-t) in Raine Island Entrance are plotted in Figure 3. The region is characterized by a near-homogeneous surface layer of about 100 m depth above a stratified lower layer; salinity is very nearly depth-independent so the density is essentially temperature controlled. In the horizontal direction, temperature and

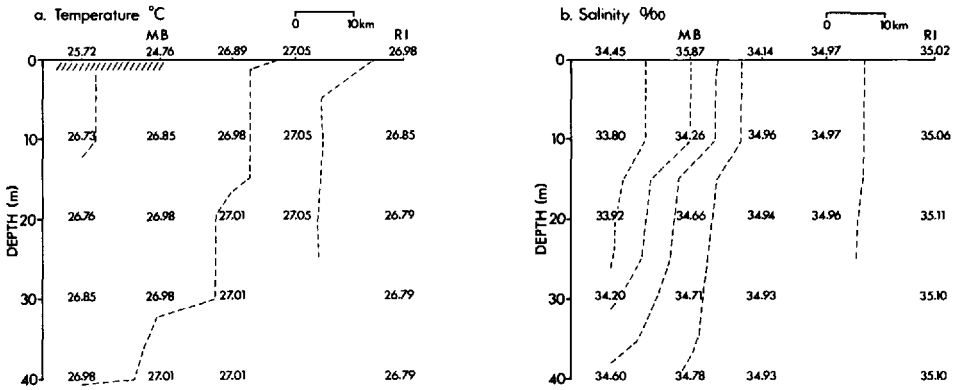

Figure 4. Sections of temperature and salinity along the CTD survey line marked by x's in Figure 1; 30 April 1982. MB Middle Banks; RI Raine Island. Area of slashed lines in (a) is surface layer of comparatively low temperatures.

salinity are almost spatially uniform within the upper layer, with differences at specified depths of about 0.5 C° and 1‰ over distances of order 50 km (Figs. 4a, b).

No nutrient data were collected at the time of the study. However, it is now well established that nutrient levels are invariably low (<1 mmol m^{-3}) in the homogeneous surface layer seaward of the shelf break and increase in a near linear manner with decreasing temperature below this layer (e.g. Thompson and Golding, 1981; Andrews and Gentien, 1982; Tomczak, 1983).

b. Temperature fluctuations. Observed temperatures for the shelf and slope moorings are plotted in Figure 5. Temperatures 5 m above the bottom on the shelf are characterized by tidal period variability with a pronounced diurnal inequality and fortnightly modulation. In addition, there is a long-term variability that appears to be related to changes in solar heating and wind-induced mixing. The r.m.s. amplitude for the record is 0.66 C° and harmonic tidal constituents account for 37% of the total variance.

The proximity of the thermocline is clearly evident in the slope record. Temperature fluctuations have a large r.m.s. amplitude of 1.87 C° and tidal constituents account for 53% of the total variance. Contrary to the shelf temperatures, there is no distinctive fortnightly modulation or apparent long period trend.

Near the end of January 1982 there was a reversal in the warming trend at the shelf location associated with the passage of a tropical cyclone. Winds recorded at Raine Island at this time were to the east and, at the peak of the storm, had daily averaged speeds in excess of 10 m s^{-1}. Daily-averaged air temperatures dropped to about 26°C compared with 28°C before and after the cyclone. As previously suggested, the onset of lower water temperatures on the shelf presumably resulted from a combination of surface cooling and enhanced vertical wind mixing. However such processes are

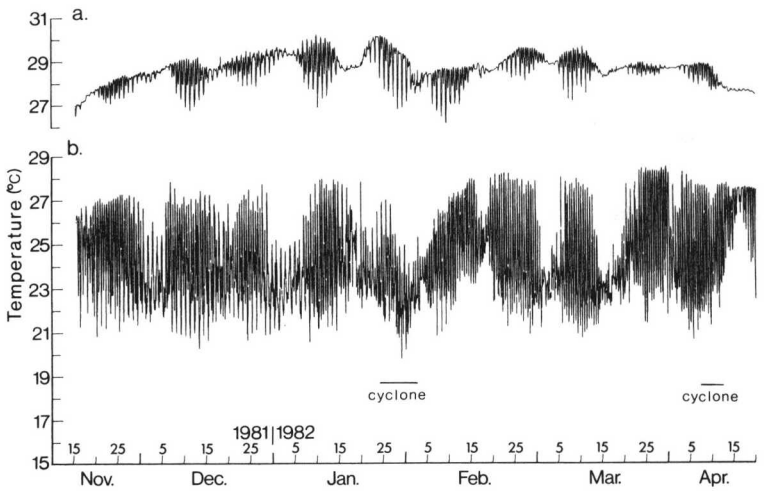

Figure 5. Half-hourly temperature observations for period 11 November 1981 to 1 May 1982. (a) shelf mooring; (b) slope mooring. Horizontal bars denote times of strong winds associated with tropical cyclones.

unlikely to explain the coincident decrease in temperature at 105 m depth at the slope mooring. We expect, instead, that the strong downchannel (eastward) winds caused a barotropic set-down and compensating baroclinic set-up at the head of the entrance, with subsequent lifting of the isopycnals over the duration of the strong winds.

c. Currents. More than 91% of the variance in the shelf current is attributable to tidal period fluctuations. A comparable value is obtained for nearby sea levels and suggests that currents in this region of the reef are largely a barotropic response to oceanic tidal forcing. As illustrated by the 15-day segment in Figure 6a, the time variable flow is almost entirely on-offshelf. The variance in the alongshore component of the flow is minimized when the offshelf direction is taken at 117.5° True (southeast), which is also the mean orientation for the semi-major axes of the principal diurnal and semidiurnal current ellipses. The mean (time averaged) flow, on the other hand, is to the southwest (215° True) at 5.3 cm s^{-1}, in apparent response to the prevailing northerly winds. Maximum daily currents are commonly around 50 cm s^{-1} and often exceed 100 cm s^{-1} during spring tides. As with temperatures, there is a significant diurnal inequality in current speed. The semi-major axes of the M_2 and K_1 constituents have amplitudes of 31.9 and 12.4 cm s^{-1}, respectively.

Observed slope currents are weaker and much more directionally variable than their shelf counterparts (Fig. 6b). Harmonic tidal constituents account for only 39% of the total variance. Moreover, well-organized flow, with speeds of 25–75 cm s^{-1}, occurs only during the ebb and gives rise to a strong eastward bias to the daily current pattern. (The variance of the alongshore component of the current is minimized when the offshore direction is specified as 90° True; i.e. eastward.)

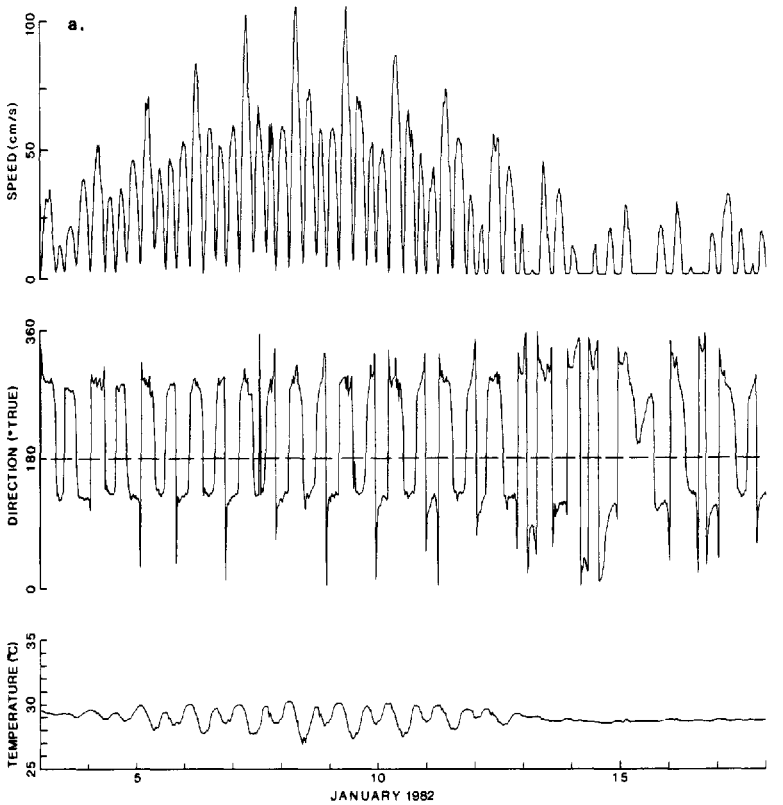

Figure 6. Fifteen day segments of the currents and temperatures at (a) shelf mooring; (b) slope mooring. Direction is in ° True (North = 0°; East = 90°).

Although our data are insufficient to delineate the apparently complex flow structure over the slope, it is possible that we have observed seaward intruding gravity currents that originate each tidal cycle during mixing of upwelled flood waters at the shelf-break. Flows of this nature have been described by various authors (e.g. Stucchi, 1980) for fjords and narrow tidal channels.

3. Results

a. Evidence for upwelling. The temperature fluctuations at the shelf and slope locations are principally the result of tidally-induced upwelling rather than horizontal advection. This contention is supported by the absence of large horizontal temperature gradients within the upper layer (e.g. Fig. 4a) and by the fact that well-stratified (thermocline) water is found below a nominal depth of 100 m (Fig. 3). Horizontal advection is, of course, responsible for moving the upwelled nutrient-rich water over the shelf once it spills over the shelf break.

If the thermocline water is to reach the 40 m deep shelf-edge, mid-slope isotherm displacements during a flood must be of order 50 m. That this is indeed the case can be

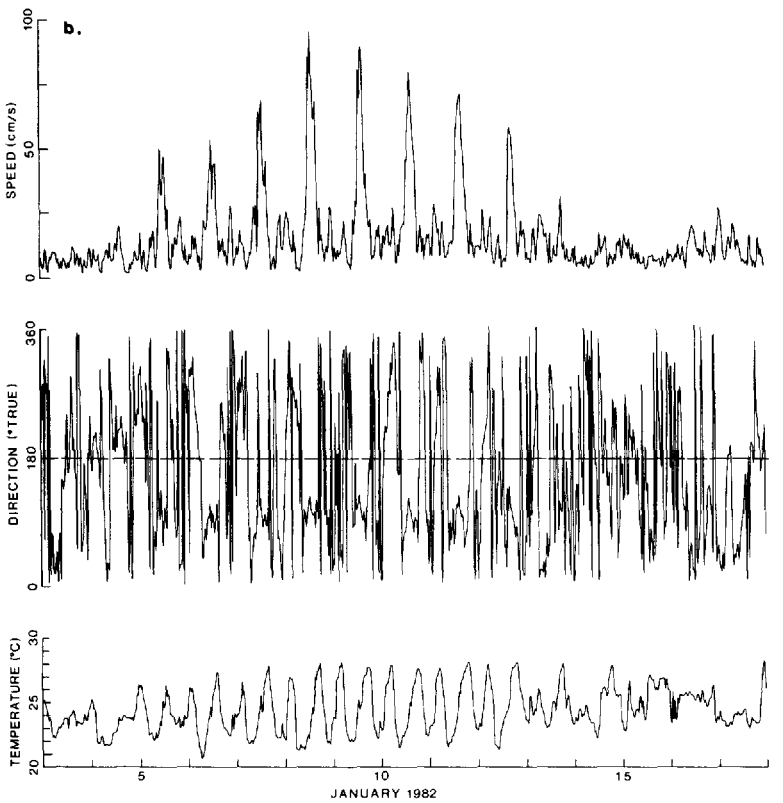

Figure 6. (Continued)

seen by comparing the slope temperatures in Figures 5b, 6b with the profiles in Figure 3. Based on a 12-hour CTD time-series near Raine Island in November 1981, we can assume that vertical motions seaward of the slope are small so that the profiles in Figure 3 are indicative of undisturbed isotherm depths within the entrance. The 'cold' 20 to 22°C water that is observed at 105 m depth on the slope must then have come from depths of 140 to 180 m; corresponding displacements are therefore in the range of 35 to 75 m. Once over the shelf-edge, the upwelled water is expected to mix with the overlying shelf water to produce a comparatively dense near-bottom layer. As a result, it is not possible to link directly the observed shelf temperature with a particular isotherm over the slope.

b. Empirical temperature-current relation. As illustrated by the temperature and current records in Figure 6a, minimum daily temperatures at the shelf mooring occur within about one hour of the turn from flood to ebb; maximum temperatures occur within one hour of the turn from ebb to flood. Consequently, temperatures and cross-shelf currents are nearly in quadrature. For a temperature T_0 of the upper layer,

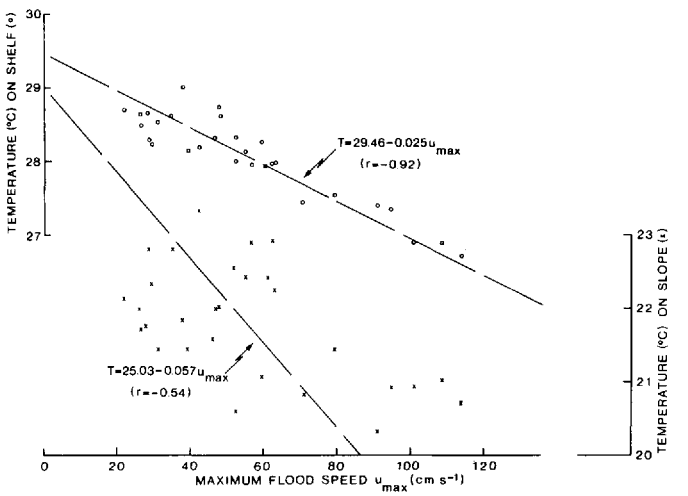

Figure 7. Minimum temperature (T_{min}) and maximum speed (u_{max}) of preceding flood current at mooring locations for period 5–20 December 1981. Similar plots are obtained at other times. Regression line has a correlation coefficient of −0.92 based on 29 half-hourly values.

there is an approximate linear relation (correlation coefficient $r = -0.92$) of the form

$$T_{min} = T_0 - a\,u_{max},\ a > 0 \tag{3.1}$$

between the minimum near-bottom temperature, T_{min}, and the maximum speed, u_{max}, of the preceding flood (Fig. 7). (No such simple relationship exists for the slope temperature and current.) The 3 to 5 h delay between T_{min} and u_{max} is due to advection in the presence of an east-west cross-shelf temperature gradient created by mixing of the upwelled water at the shelf break.

c. Eddy heat flux. The across-shore and alongshore components of the eddy heat flux per unit cross-sectional area are (e.g. Bryden *et al.*, 1980):

$$\rho C_p\,\overline{u'T'} = \rho C_p\,\overline{(u - \bar{u})\,(T - \bar{T})}, \tag{3.2a}$$

$$\rho C_p\,\overline{v'T'} = \rho C_p\,\overline{(v - \bar{v})\,(T - \bar{T})}, \tag{3.2b}$$

in which u, v are the across and alongshore velocity components, T is the temperature, C_p is the specific heat of seawater and $(-)$ denotes the time average over the length of the record. In order to determine the reliability of the heat flux estimates, we have broken the temperature and velocity records into sequential 512-hour segments and computed the fluxes for each segment. The resulting mean and standard deviations for the along- and cross-shore components at the two mooring locations are presented in Table 1 together with the corresponding values for the correlation coefficients,

$$\overline{u'T'}/(\overline{u'^2}\,\overline{T'^2})^{1/2},\ \overline{v'T'}/(\overline{v'^2}\,\overline{T'^2})^{1/2}.$$

Table 1. Estimates of the cross-shelf and along-shelf components of the eddy heat flux (3.2a,b) and associated correlation coefficients for the shelf and slope mooring sites. At the shelf mooring, off-shelf is toward 117.5° True; for slope mooring off-shelf is toward 90° True. Means and standard deviations based on seven 512-hour segments of the total records.

	Eddy heat flux		Correlation coefficient	
Location	Across cal cm^{-2} s^{-1}	Along cal cm^{-2} s^{-1}	Across	Along
shelf	0.79	−0.42	0.039	−0.046
	(±1.01)	(±0.56)	(±0.046)	(±0.193)
slope	9.40	−1.59	0.331	−0.159
	(±4.86)	(±1.39)	(±0.095)	(±0.198)

In all cases estimates are found to be insensitive to the record length in the range of 506 to 518 hours, corresponding to roughly 20 to 21 diurnal cycles.

The mean cross-shelf component of the eddy heat flux is seaward at both mooring locations with the shelf value (0.79 cal cm^{-2} s^{-1}) an order of magnitude smaller than the slope value (9.40 cal cm^{-2} s^{-1}). The small correlation coefficient for the shelf location indicates that temperature and current fluctuations are close to quadrature and that linear regression explains less than one percent of the covariance. In contrast, linear regression accounts for more than 10% of the covariance at the slope location. The larger flux over the slope is presumably due to seaward flowing density currents that originate during mixing of upwelled water over the outer shelf. In this case, the daily ebb current will carry relatively warm water to the depth of the thermocline. The significance of this transport to the overall heat balance in the region will depend on the width of density current. We also note that the alongshore heat fluxes are to the south at both locations and that the small correlation coefficients are indicative of advection in the presence of a mean north-south temperature gradient.

An estimate of the vertically integrated heat flux associated with the upwelling is obtained by multiplying the across-shelf fluxes in Table 1 with a depth H of upwelled water on the shelf. For a reasonable guess $H \sim 10$ m (e.g. Andrews and Gentien, 1982), we obtain a seaward eddy heat flux on the shelf of 0.8 (±1.0) × 10^3 cal cm^{-1} s^{-1}. Using this depth of the thickness of the slope current yields a seaward flux of 0.9 (±0.5) × 10^4 cal cm^{-1} s^{-1}. These estimates may be compared with the depth-integrated onshore eddy heat flux of 1.8 × 10^4 cal cm^{-1} s^{-1} derived by Bryden *et al.* (1980) for 100 m of water on the Oregon shelf and the offshore eddy heat flux of 4.5 × 10^3 cal cm^{-1} s^{-1} determined by Richman and Badan-Dangon (1983) for 73 m of water on the Northwest Africa shelf.

To simulate flux conditions at the shelf break, we lag the shelf temperature record by 3 h (90° at diurnal periods) relative to the cross-shelf current record. This yields a relative maximum seaward eddy heat flux of 1.0 (±0.4) × 10^4 cal cm^{-1} s^{-1} which is almost identical to the heat flux across the slope and is presumably representative of the flux induced by upwelling at the shelf break where u and T are expected to be

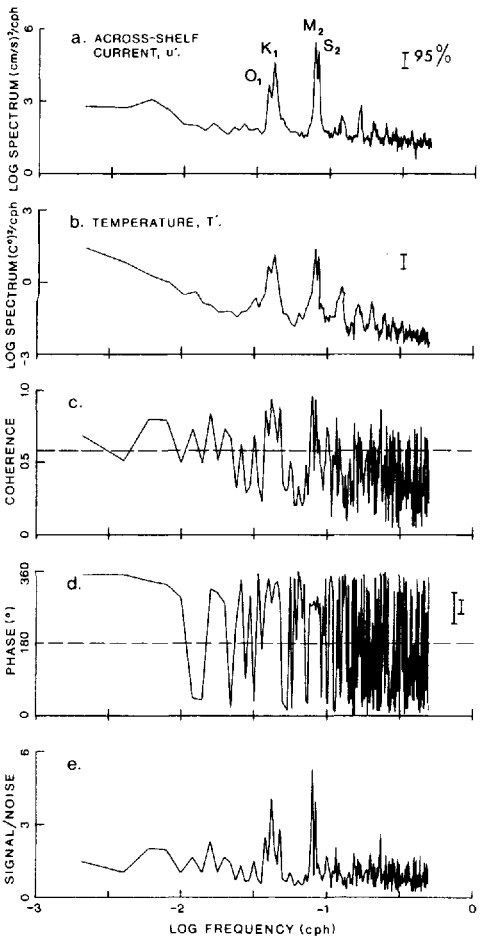

Figure 8. Spectra and coherences for cross-shelf (u') and temperature (T') fluctuations on the shelf. (a) u' spectrum; (b) T' spectrum; (c) Coherence amplitude with 95% confidence limit (dashed line); (d) Coherence phase; (e) Signal-to-noise level. Vertical bars denote 95% confidence levels. Bandwidth = 0.002 cph with 16 degrees of freedom. Phase error bars are derived for phase angle standard deviations of 50° and 100°.

in-phase. The large correlation coefficient 0.58 ± 0.17 in this case means that the linear regression of u, T accounts for over 30% of the variance. If this estimate is indeed representative of the shelf break, then the flux divergence between the shelf and shelf break must be compensated by a surface heat flux and/or an onshore flux in the upper portion of the water column. Neither processes can be resolved by the present data set.

d. Heat flux versus frequency. The spectra of the heat flux components u', T' for the shelf mooring are plotted in Figure 8 along with the coherence and signal-to-noise (SN) ratio. [Signal-to-noise is defined as coherence ÷ $(1\text{-coherence}^2)^{1/2}$.] The fluctu-

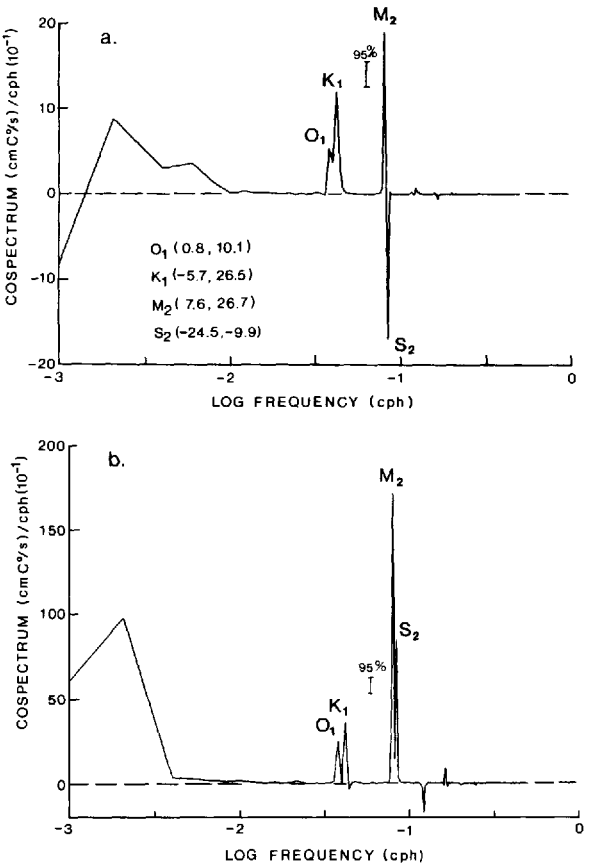

Figure 9. Temperature (T') and current (u') cospectra for (a) shelf and (b) slope mooring location. Solid 95% confidence error bars are based on conventional statistics using variances over the band 0.030 to 0.052 cph; the bracketed values in (a) give the maximum and minimum values for each major tidal constituent based on phase uncertainty associated with harmonic constituents (cf Fig. 10). The latter are obtained by multiplying the flux extrema derived from the harmonic constituents by the ratio cospectral flux estimate ÷ harmonic flux estimate.

ations are mainly confined to the principal diurnal (O_1, K_1) and semidiurnal (M_2, S_2) tidal frequencies. Largest coherences and SN levels occur within these bands with current fluctuations leading temperature fluctuations by approximately 270° at semidiurnal frequencies and by 270–300° at diurnal frequencies. The results for the slope mooring are similar to those on the shelf except that current-temperature leads are typically around 300° at all tidal frequencies.

Because the temperature and current signals in Figure 8 are nearly in quadrature at semidiurnal frequencies, we expect diurnal frequency motions to be the principal contributors to the cross-shore heat flux. At the slope location, all major tidal bands should contribute to the flux. These expectations are borne out by the u', T' cospectra for the two mooring sites (Figs. 9a, b). The solid error bars in these figures are based on

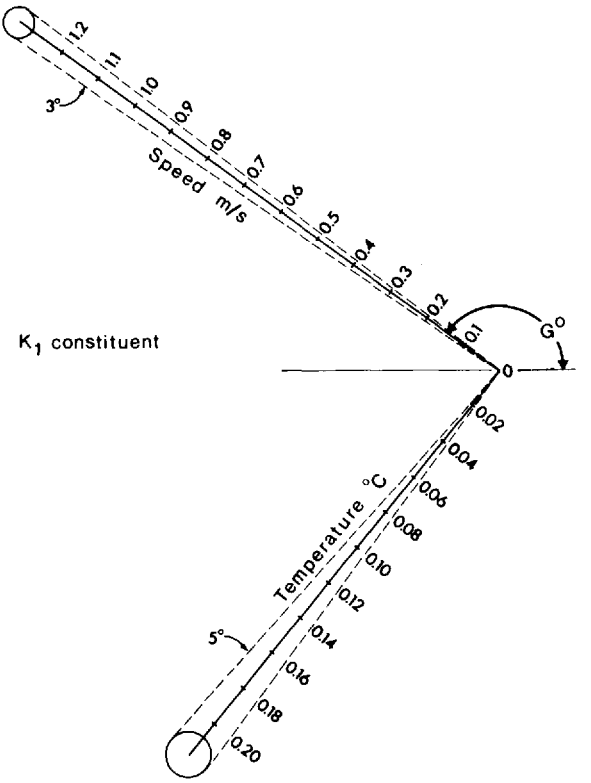

Figure 10. Solid lines give amplitudes and phases (G°) of the K_1 temperature and tidal current constituents for the shelf location based on full record length of 154 days. Radius of circle of standard error in each case is derived from the spectral background level near the diurnal frequency band. Also shown are the maximum angles subtended by the error circles.

conventional statistics (using variance levels near the diurnal frequencies) and suggest that the positive fluxes over the shelf are significant at diurnal frequencies. However, conventional statistics are not generally applicable when fluctuations are dominated by large amplitude tidal motions. Consequently, we have also obtained error estimates (bracketed values) for the shelf location by estimating the uncertainty in the phases of the major flux constituents. As exemplified by the case for the K_1 frequency in Figure 10, the variations in the phases of temperature and current are assumed to be statistically independent and to derive from the background "noise" level near the tidal bands. The resultant extremae for the cross-shelf fluxes in Figure 9a suggest that the nominal values are marginally significant at diurnal frequencies.

The prominence of the major tidal bands in Figures 9a, b indicates that cross-shore heat fluxes can be estimated from the products $\frac{1}{2}\rho C_p u_j T_j \cos\phi_j$, where the amplitudes u_j, T_j and relative phases ϕ_j of the current and temperature records correspond to the main tidal frequencies, j. To obtain the above products, the current and temperature records have been divided into a series of seven 29-day segments and standard

Table 2. Cross-shelf heat flux $\rho C_p uT$ (cal cm^{-2} s^{-1}) for current meter locations. a. Flux based on harmonic constituents from seven 29-day segments. b. Flux determined by multiplying cospectra at selected frequency bands by the bandwidth 0.002 cph. $\rho = 1.025 \times 10^3$ kg m^{-3}.

a. Cross-shore heat flux (Harmonic analysis)

	Tidal constituent and frequency				
Location	(0.0387 cph)	(0.0418 cph)	(0.0805 cph)	(0.0833 cph)	Ratio: diurnal to semidiurnal
shelf	+0.14 ± 0.23	+ 0.30 ± 0.26	+ 0.44 ± 0.25	−0.42 ± 0.25	17.2
slope	+0.53 ± 0.33	+ 0.74 ± 0.32	+ 3.25 ± 2.49	+1.82 ± 1.77	0.2

b. Cross-shore heat flux (cospectral analysis)

	0.0380 cph	0.0420 cph	0.0800 cph	0.0840 cph	
shelf	+0.14 ± 0.07	+0.31 ± 0.07	+0.40 ± 0.07	−0.33 ± 0.07	6.4
slope	+0.52 ± 0.25	+0.69 ± 0.25	+3.84 ± 0.25	+1.86 ± 0.25	0.2

harmonic analysis applied to each segment. (Records of 29-day duration permit resolution of the principal daily and fortnightly tidal components; because the temperature records are strongly modified by wind and heating effects, inferred tidal constituents have not been used.) The means and standard deviations for both the shelf and slope locations are presented in Table 2a. For comparison, Table 2b lists the corresponding values of the fluxes obtained by multiplying the cospectra in Figures 9a, b by the bandwidth (0.002 cph); standard deviations are derived from the standard error bars in the figures. The residual cross-shore fluxes, obtained by subtracting the harmonic (tidal) components from each 29-day record, are +0.18 (±0.54) cal cm^{-2} s^{-1} at the shelf location and +2.15 (±1.22) cal cm^{-2} s^{-1} at the slope location. These values are approximately a factor of five smaller than the corresponding tidal fluxes in Table 2a.

Based on the cospectra in Figure 9a, diurnal and semidiurnal oscillations at the shelf location account for 69% and 12%, respectively, of the integrated covariance (total heat flux) while periods longer than 5 days account for slightly more than 5%. The low value for the semidiurnal band is due to the ~90° phase difference between the temperature and current fluctuations at this frequency. We attach no physical meaning to the opposite signs of the heat fluxes at the M_2 and S_2 frequencies but link this to small differences in phase near 90°; in this case, only the band-averaged flux has meaning. At the slope location (Fig. 9b) the roles are reversed with 12% and 61%, respectively, of the heat flux in the diurnal and semidiurnal bands. Periods longer than 10 days account for 22% of the covariance.

e. Nutrient fluxes. To obtain the onshore nutrient flux associated with the upwelling, we assume a linear relationship $n \sim -bT$ between inorganic nutrient concentration and temperature below the surface homogeneous layer. Andrews and Gentien (1982),

for example, state that nitrate concentrations, n_n, for stations beyond the shelf break near Myrmidon Reef (18.5S) satisfy $n_n = 29.7 - 1.20\ T$ mmol m^{-3} for temperatures greater than 12°C. Similarly, nutrient data compiled by Tomczak (1983) for the open Coral Sea off the east Australian coast indicate that, for $10° < T < 25$°C, nitrate, phosphate and silicate levels are very approximately given as (with T in °C):

$$n_n = 30.2 - 1.2\ \mathrm{T\ mmol\ m^{-3}}, \tag{3.3a}$$

$$n_p = 2.2 - 0.09\ \mathrm{T\ mmol\ m^{-3}}, \tag{3.3b}$$

$$n_s = 17.6 - 0.8\ \mathrm{T\ mmol\ m^{-3}}. \tag{3.3c}$$

The onshore eddy nutrient fluxes, $\overline{u'n'}$, are then found by multiplying the offshore eddy heat fluxes in Table 1 by $b/\rho C_p$, where b is a particular value for the slope from the previous nutrient-temperature relations. Results for the shelf mooring location are:

$$\overline{u'n'_n} \sim -0.92\ (\pm 1.18) \times 10^{-2}\ \mathrm{mmol\ m^{-2}\ s^{-1}}, \tag{3.4a}$$

$$\overline{u'n'_p} \sim -0.69\ (\pm 0.89) \times 10^{-3}\ \mathrm{mmol\ m^{-2}\ s^{-1}}, \tag{3.4b}$$

$$\overline{u'n'_s} \sim -0.61\ (\pm 0.79) \times 10^{-2}\ \mathrm{mmol\ m^{-2}\ s^{-1}}. \tag{3.4c}$$

Flux estimates for the slope mooring exceed those in (3.4) by an order of magnitude.

The head of Raine Island Entrance has a width of about 20 km. This, combined with the fluxes in (3.4) and an assumed layer thickness of 10 m, yields mean total onshore fluxes of: 1.84 mol s^{-1} (5.80×10^7 mol yr^{-1}) for nitrate, 0.14 mol s^{-1} (0.44×10^7 mol yr^{-1}) for phosphate and 1.22 mol s^{-1} (3.85×10^7 mol yr^{-1}) for silicate. Integration of the across-shelf current with time shows that flood currents could advect upwelled water 10–15 km onshore from the shelf break. On this basis, the annual nitrate input to the reef near Raine Island Entrance is around 20–30 mmol m^{-3} which is comparable to the value of 20 mmol m^{-3} obtained by Andrews and Gentien (1982). Equally impressive amounts are obtained for phosphate and silicate. However, because nontidal currents and associated mixing processes are expected to distribute the nutrients over an even greater area of the shelf, such large inputs should be considered as upper limits. The above discussion is not meant to imply that only a net advective transport of nutrients is important to the reef ecology. On the contrary, the fact that the continental shelf near Raine Island Entrance is inundated with a layer of relatively cold water on each flood suggests that organisms of the outer reef are regularly supplied with nutrients irrespective of any net cross-shelf transport. Nutrients removed by the organisms during each tidal cycle are presumably resupplied to the water column on the ebb through such processes as vertical mixing and alongshore advection. Ten kilometers or so shoreward of the shelf break, nutrient fluctuations are expected to be of the order of the observed r.m.s. temperature variations of 0.66 C° multiplied by the slopes 'b' in (3.3a, c). For example, nitrate variances should be about 0.79 mmol

m^{-3}. Near the shelf break, on the other hand, nutrient fluctuations are expected to be closer to the r.m.s. slope temperature fluctuations 1.86 C° times b.

f. Upwelling mechanisms. Thompson and Golding (1981) present a tidally-induced upwelling model that is applicable to Raine Island Entrance. Let x be the distance seaward of the shelf break and u the corresponding velocity component. From continuity and ignoring possible lateral confinement of the flow due to reefs, we obtain

$$u(x) = \hat{u}_0 \hat{H}_0/H(x) \tag{3.5}$$

where $H(x)$ is the water depth over the slope and ($\hat{}$) refers to values on the shelf. We assume that at some depth over the slope the flood current speed will exceed the maximum phase speed c of internal gravity waves in the thermocline. Because the flow is supercritical shoreward of this position, no wave-induced shear exists between the homogeneous surface layer and the stratified water below. Therefore, within the regime of supercritical flow, thermocline water is "sucked" onto the shelf. The problem reduces to determining where the phase speed of internal waves matches the flood speed.

Based on a WKB approximation and assuming a surface layer of constant density ρ_0, Thompson and Golding find that the fastest phase (and group) speeds for internal waves on the slope occur for wavenumbers $k \to 0$. Then c is determined by the dispersion relation,

$$\frac{N}{c} D + \tan \frac{N}{c} d = 0, \tag{3.6}$$

in which $N = [-g/\rho\ (d\rho/dz)]^{1/2}$ is the Brunt-Väisälä frequency, D and $d(x)$ are the respective thicknesses of the homogeneous and stratified layers, g is gravity and $\rho(z)$ is the density as a function of depth. If we fit an exponential density structure, $\rho(z) = \rho_0 \exp[-\alpha(z + D)]$, to the well-stratified regions $D \leq |z| \leq 200$ m in Figure 3, we obtain

$$N = (g\alpha)^{1/2} \sim 1.3 \pm 0.1\ (10^{-2})\ s^{-1}$$

where D has values of 100 and 140 m.

Estimates of $c(d)$ for $N = 0.13\ s^{-1}$ and the two values of D are plotted in Figure 11 along with representative values of $u(x)$ from (3.5). Intersections of the curves give the maximum penetration depth of the upwelling process; all water shallower than these depths should be drawn onto the shelf. For commonly observed flood speeds ($u_0 \sim 50\ cm\ s^{-1}$), the model predicts that upwelling is from a maximum depth of 20 m below the surface homogeneous layer whereas for large spring tides ($u_0 \gtrsim 130\ cm\ s^{-1}$) it is from a depth of 40 to 50 m below the surface layer.

An alternative upwelling model is presented by Stommel *et al.* (1973). The model

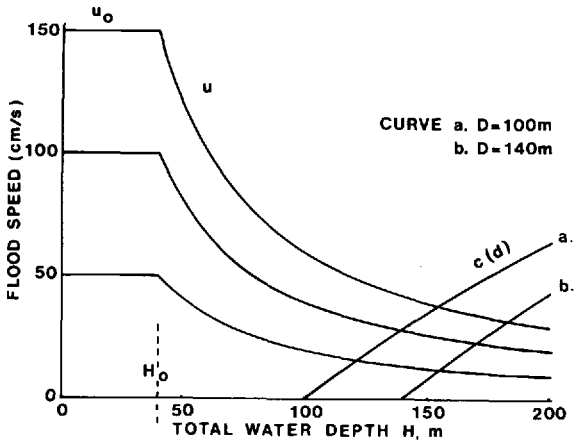

Figure 11. Internal wave speed $c(d)$ and cross-shelf flood speed $u(x)$ as a function of total water depth $H(x)$ for two depths D of the upper homogeneous layer. x is distance seaward of the shelf break.

assumes that density is conserved along streamlines, that velocities are negligible far from the region of minimum depth and that there is a vertical hydrostatic balance. Bernoulli's equation is then applied to two vertically separated streamlines (Fig. 12) to obtain expression for the near-bottom current u_1 at depth z_1 at the shelf-edge;

$$(1 + \delta)\, u_1^2 = u_1^{*2} - \Sigma, \tag{3.7}$$

where u_1^* is the current at depth $|\, z_1^* \,| < |\, z_1 \,|$ at the shelf edge, $\delta = (\rho_0 - \rho_0^*)/\rho_0$ is relative density difference in the interior and

$$\Sigma = 2g\delta\, [z_0 - z_1 - \epsilon_0(z_0 - z_0^*) + \epsilon_1(z_1 - z_1^*)]. \tag{3.8}$$

In (3.8), z_0 and z_0^* are the depths of the streamlines in the interior and

$$\epsilon_0 = (\bar{\rho}_0 - \rho_0^*)/(\rho_0 - \rho_0^*),\ \epsilon_1 = (\bar{\rho}_1 - \rho_1^*)/(\rho_0 - \rho_0^*). \tag{3.9}$$

Here, ρ_0^* and ρ_1^* are the densities at depths z_0^* and z_1^*, respectively, $\bar{\rho}_1$ is the vertical mean between the shelf depths z_1 and z_1^* and $\bar{\rho}_0$ is the corresponding value for the slope depth range z_0 to z_0^*.

Upwelling occurs if (3.7) is positive. As a consequence, $\Sigma^{1/2}$ from (3.8) gives the threshold flood speed needed to lift thermocline water onto the shelf. The speeds in Figure 13 are for various depths z_0 of the isopycnals near Raine Island (Fig. 3) roughly 15 km from the shelf. In deriving the estimates, we set $\epsilon_1 = 0$, since ρ_1 is very nearly uniform with depth even during upwelling, and have taken ϵ_0 between 0.3 and 0.6 in order to span the range determined by measured values of $\bar{\rho}_0$. We assume also that $\rho_0^* = \rho_1^*$. (The value $\epsilon_0 = 0.5$ is appropriate to a two-layer or linear density structure; Stommel *et al.* use 0.6.) The sea surface is a streamline so we choose $z_0^* = 0$ while $z_1 = 40$ m is logically the depth of the shelf. For the November CTD survey (Fig. 3), we

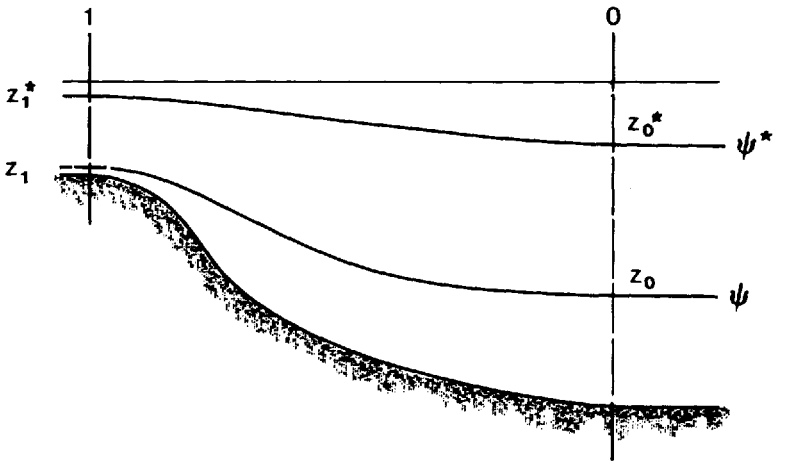

Figure 12. Definitions for upwelling model. ψ denotes streamlines.

ignore the thin (<5 m) layer produced by winter precipitation and specify $\rho_0^* = 1.0231$ gm cm^{-3} based on the density at 5 m depth.

Even for the worst case, $\epsilon_0 = 0.3$, the measured flood currents of 50–130 cm s^{-1} are capable of raising the thermocline to the shelf edge. Moreover, the depth penetration of the upwelling is comparable to that of the previous model (Fig. 11). Both models produce coldest (deepest) water over the shelf break at maximum flood and both are presumably invalid over the shelf where turbulent mixing is taking place.

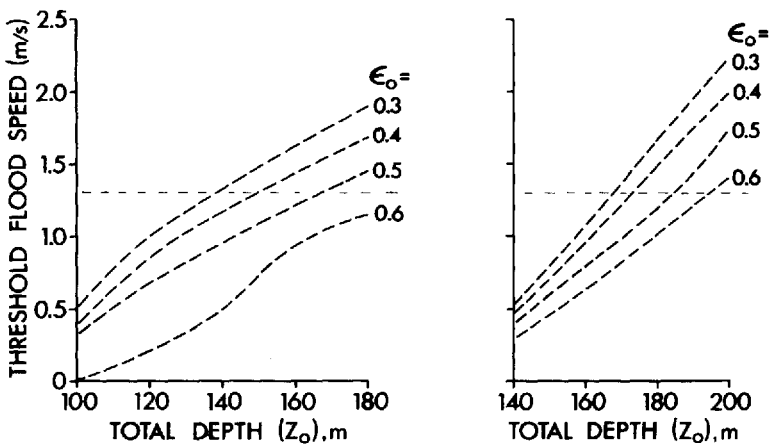

Figure 13. Values of the threshold flood current speed $\Sigma^{1/2}$ (m s^{-1}) from (3.8) needed to raise isopycnals of depth z_0 in Raine Island Entrance to the depth $z_1 = 40$ m of the shelf edge. ϵ_0 is the fractional density (3.9). Values above the horizontal line exceed the observed maximum flood speeds over the shelf. Results derived for November 1981 CTD survey and April 1982 survey (Fig. 3).

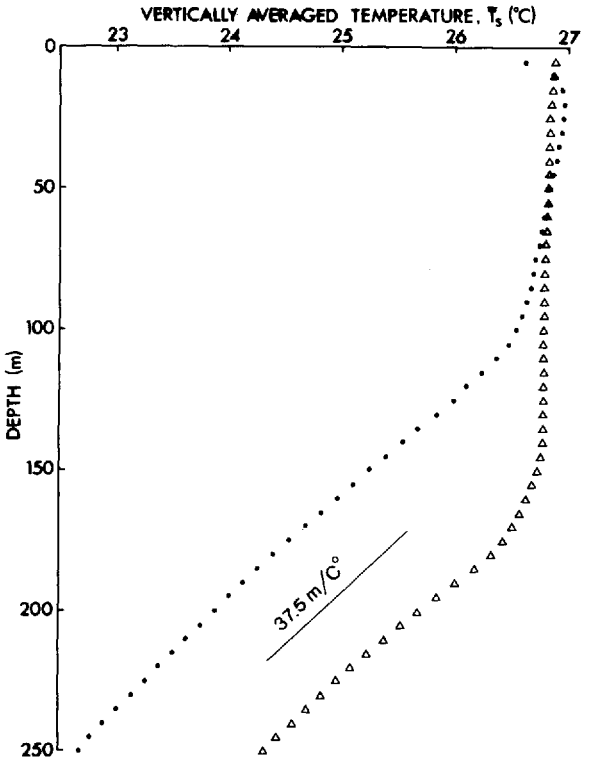

Figure 14. Vertically averaged temperature profiles $\bar{T}_s$ (3.10) for the November 1981 and May 1982 temperature profiles from Raine Island Entrance (Fig. 3). Shown is the mean slope $(d\bar{T}_s/dz)^{-1}$ below the surface homogeneous layer.

g. Comparison with observation. The results of the models may be compared with an estimate of the maximum upwelling depth, z_0, obtained by equating the change (ΔT) in the observed shelf temperature T with the change in the vertically integrated slope temperature

$$\bar{T}_s(z_0) = z_0^{-1} \int_0^{z_0} T_s(z)dz. \tag{3.10}$$

In particular,

$$z_0 = D + (d\bar{T}_s/dz)^{-1} \Delta T \tag{3.11}$$

where, as before, D is the depth of the surface homogeneous layer. Plots of (3.10) for the temperature profiles obtained at the beginning and end of the current measurements (Fig. 3) are presented in Figure 14. Except for a transition zone beneath the mixed surface layer, the slope at both times was

$$d\bar{T}_s/dz = 0.027\ \text{C}^\circ\ \text{m}^{-1} \tag{3.12}$$

and D ranged from 100 m at the start to 140 m at the end of the observations.

From Figure 7, we find $\Delta T = -0.025\ \Delta u_{\max}$. Eqs. (3.11) and (3.12) then yield

$$z_0 - D = 0.93 \times 10^2\ (u_{\max} - u_0)$$

where $z_0 - D$ is in meters and $u_{\max}$, u_0 are in m s^{-1} and where, according to the results in Figure 7, u_0 must exceed approximately 0.4 m s^{-1} before there is a significant change in shelf temperature and, hence, upwelling depth. Using the value $u_{\max} \sim 1.3$ m s^{-1} for large spring tides, we find

$$z_0 - D \simeq 85\ \text{m},$$

which is considerably greater than the value of 50 m estimated for the Thompson and Golding model (Fig. 11) and the value of 50–60 m for the Stommel *et al.* model (Fig. 12). On this basis, the time-independent models appear to underestimate the upwelling depth.

4. Summary and conclusions

The analytical models presented in this paper indicate that observed tidal currents at the head of Raine Island Entrance are sufficiently strong to draw cold, nutrient-rich thermocline water from the slope to the shelf. For commonly observed flood speeds of 50 cm s^{-1}, the water can upwell from as deep as 20 m below the homogeneous surface layer; for maximum observed speeds of 130 cm s^{-1} it can upwell from more than 50 m below this layer. Vertical excursions of these magnitudes are verified by the temperature measurements over the slope a few kilometers from the shelf break. Winds, quasi-geostrophic oceanic currents and baroclinic tides may also have an influence on isotherm depths over the slope, though none of these mechanisms is addressed in this paper.

According to the upwelling models, minimum near-bottom temperatures in the vicinity of the shelf break coincide with times of maximum flood. The tides are of the mixed variety so there is a diurnal inequality in the values of consecutive temperature minimums. As the upwelled water crosses the outer shelf, it presumably mixes with the overlying homogeneous water to produce cross-shelf gradients in temperature and nutrient concentration. It is the onshore advection of this water which leads to the 0.66 C° (r.m.s.) temperature fluctuations observed at the shelf mooring ~8 km from the shelf edge. Integration of the flood speeds with time yields water parcel excursions of 10–15 km, and is taken as a measure of the cross-shelf distances that nutrient levels are expected to be directly enhanced by tidally-induced upwelling. Nontidal currents (e.g. wind generated currents) may further augment the onshore transport of nutrients to the reef lagoon (Andrews and Gentien, 1982).

The upwelling results in a net seaward eddy heat flux, $\rho C_p \overline{u'T'}$, of 0.79 ($\pm$1.01) cal

$cm^{-2}\,s^{-1}$ over the shelf. About 69% of the flux is due to diurnal period oscillations and 12% to semidiurnal period oscillations. At the slope mooring, the offshore eddy heat flux is much larger, 9.40 (±4.86) cal $cm^{-2}\,s^{-1}$, and the importance of the major frequency bands reversed. Here, 61% of the flux is in the semidiurnal band and only 12% in the diurnal band. In addition, a significant portion (22%) of the flux is associated with low frequency motions with periods in excess of 10 days. We attribute the comparatively large eddy flux on the slope to seaward flowing density currents that form initially over the outer shelf during each flood. On the ebb, the denser water sinks into Raine Island Entrance to produce a fairly intensive "jet" whose penetration depth is necessarily limited by the stably stratified thermocline.

Using empirical nutrient-temperature curves provided by Tomczak (1983) we were then able to convert the seaward eddy heat flux to onshore nutrient fluxes. These estimates are very approximate but give an indication of the magnitudes of nitrate, silicate and phosphate that are brought onto the shelf through upwelling. Our findings support the notion that tidal currents alone are able to enrich the near-bottom waters over the outer shelf, at least in the vicinity of major passages. Whether nontidal processes are responsible for more widespread distribution of the nutrients remains an open question, though it seems reasonable that individual passages through the Barrier Reef act as daily "pulsating" source functions whose integrated nutrient input is essential to the welfare of the reef.

Acknowledgments. We wish to thank the Australian Institute of Marine Science for conducting the field work and providing generous support during all stages of the experiment. Captain John Futcher of the *Lady Basten* and Mr. Ray McAllister are thanked for their considerable effort during the field operations. We also acknowledge the kind assistance of David van Senden, Dr. Jason Middleton, Tim Horn, Martin Jones and Greg Nippard. The data analysis was performed expertly by Joe Linguanti. Nutrient data were generously supplied by Dr. Matthias Tomczak with the kind assistance of Dr. Rory Thompson. Dr. Chris Garrett and Dr. Barry Ruddick are thanked for providing valuable advice on numerous aspects of the manuscript. The authors also benefitted from useful discussions with Drs. Andrew Bennett and Howard Freeland.

APPENDIX

Across shelf eddy heat flux (cal cm^2/s) for different averaging times (averages based on seven consecutive periods). Normal value (i.e. value used in paper = 512 hours).

Record length (hours)	Value (Mean + SD)	% Difference from nominal
506	0.72 1.04	8.9
509	0.75 1.34	5.1
512	0.79 1.01	—
515	0.79 1.11	0
518	0.80 1.04	1.3

REFERENCES

Andrews, J. C. and P. Gentien. 1982. Upwelling as a source for the Great Barrier Reef ecosystems: a solution to Darwin's question? Mar. Ecol.–Prog. Ser., *8,* 257–269.

Bryden, H. L., D. Halpern and R. D. Pillsbury. 1980. Importance of eddy heat flux in a heat budget for Oregon coastal waters. J. Geophys. Res., *85,* No. C11, 6649–6653.

Garrett, C. 1979. Topographic Rossby waves off east Australia: identification and role in shelf circulation. J. Phys. Oceanogr., *9,* 244–253.

Maxwell, W. P. H. and J. P. Swinchatt. 1970. Great Barrier Reef: regional variation in a terrigeneous-carbonate province. Bull. Geol. Soc. Am., *81,* 691–724.

Orr, J. P. 1933. Scientific report of the Great Barrier Reef expedition, 1928–1929. British Mus. (Nat. Hist.) II, 37–86.

Pickard, G. L., J. R. Donguy, C. Henin and F. Rougerie. 1977. A review of the physical oceanography of the Great Barrier Reef and Western Coral Sea. Australian Inst. Mar. Sc. Monograph Ser., *2,* 134 pp.

Richman, J. and A. Badan-Dangon. 1983. Mean heat and momentum budgets during upwelling for the coastal waters off northwest Africa. J. Geophys. Res., *88,* 2626–2632.

Stommel, H., H. Bryden and P. Mangelsdorf. 1973. Does some of the Mediterranean outflow come from great depth? Pageoph, *105,* 879–889.

Stucchi, D. J. 1980. The tidal jet in Rupert-Holberg Inlet, *in* Fjord Oceanography, H. J. Freeland, D. M. Farmer and C. D. Levings, eds., Plenum Publishing Co., New York, 491–497.

Thompson, R. O. R. Y. and T. J. Golding. 1981. Tidally induced 'upwelling' by the Great Barrier Reef. J. Geophys. Res., *86,* 6517–6521.

Tomczak, M. Jr. 1983. Coral Sea water masses, *in* Proceedings Great Barrier Reef Conference, James Cook University, Townsville, J. T. Baker, R. M. Carter, P. W. Sammarco and K. P. Stark, eds., 461–466.

Wolanski, E. and G. L. Pickard. 1983. Upwelling by internal tides and Kelvin waves at the continental shelf break on the Great Barrier Reef. Austral. J. Mar. Freshwater Res., *34,* 65–80.

Received: *24 January, 1983;* revised: *30 April, 1984.*